BEDLOAD DISCHARGE MEASUREMENT IN ACTUAL RIVER WITH MBES AND ADCP

KOICHI TSUCHIDA
Fukuda Hydrologic Center, Sapporo, Japan, k-tsuchida@f-suimon.co.jp

MASAHIRO HASHIBA
Fukuda Hydrologic Center, Sapporo, Japan, hashiba@f-suimon.co.jp

ABSTRACT

Bedload discharge is important to understand the sediment dynamics in the basin and to verify to the numerical analysis of river bed fluctuating. However, it was difficult to install the bedload sampler on the river bed during high flow and there was involved uncertain data. In this study, we conducted the observation of bedload migration and river bed form using two acoustic devices in an actual river which were the ADCP for bedload velocity measurement and Muti-Beam Echo Sounder(MBES) for detail bathymetry measurement. The boat with an acoustic device was moved from downstream to upstream repeatedly every 10 minutes for 1.5 hours. Next, by using measured data which were bed waveforms, bed migration, we evaluated bedload discharge measurement methods in the actual river. The sand waveform estimated by MBES that the average wavelength was 3.5m, the average wave height was 0.2m. Moreover, the MBES data were estimated the moving speed of the sand waves using the space-time image, the result was from 0.03 m/min to 0.11 m/min. Finally, regarding the bedload discharge, we compared two different methods. The first one is the bedform migration which was the function of the wave height and the wave migration speed by MBES proposed by Kikkawa (1985). The second one is the method using the bedload velocity of ADCP proposed by Koseki et al. (2016). As a result, the bedload discharge was close to similar to each other. Therefore, it was shown that it is possible to estimate the bedload discharge using ADCP without directly sampling the bedload.

Keywords: *MBES, ADCP, Sand wave, Actual river, Bedload*

1. INTRODUCTION

Bedload discharge is an essential factor of sediment transport. It is useful to understand the sediment dynamics in the basin and to verify to the numerical analysis of river bed fluctuation. The bedload sampler was developed since the 1960s. However, because it was challenging to install the sampler on the river bed during high flow, there was involved uncertain data. Rennie (2002) has been studying the sediment load by the ground movement speed using the bottom tracking of ADCP as a monitoring technique for estimating sediment transport during flooding. Ramooz(2010) compared with ground speed measured using ADCP bottom tracking function and moving digital image of the particle. On the other hand, Yorozuya et al. (2010) developed a methodology to estimate the bedload rate with ADCP. Uehara et al. (2018) proposed a calculation method of the bedload discharge using the bottom track velocity measured by ADCP experimenting with a movable bed. Muste et al. (2015, 2016) developed the method for the bedload in actual rivers using the Acoustic for Mapping Velocimetry. Abraham et al. (2010,2011) proposed the algorithm for evaluation of bed dynamics using MBES. It showed that the correlation between ground speed due to bottom tracking of ADCP and Bedload velocity is higher in the case of sand with small grain size. Koseki et al. (2016) updated the method by Yorozuya et al. (2010), which estimates the shear stress by the bedload velocity. As a result, the bedload discharge, as well as the local shear velocity, has become possible by implementing the bottom track function of ADCP and the bedload function of Egashira (1997). In this study, the authors conducted the field measurement with the MBES and ADCP mounted on a manned-control boat in an actual river. Measured by using data, which are river bed shape, bedform migration, and bedload discharge, we evaluated sediment measurement methods of Koseki et al. (2016) in the actual river.

2. METHOD OF FIELD OBSERVATION

2.1 Field information

The authors conducted the field study in the Ishikari River during the snow melting season, which is April 24-25, 2019. Figure 1 shows the location of the Hokkaido, river basin of the Ishikari River, and the gauging point. The total catchment area of the Ishikari River is 14300 km2. This gauging point located in the middle of the river, whose distance from the sea is 26.5 km.

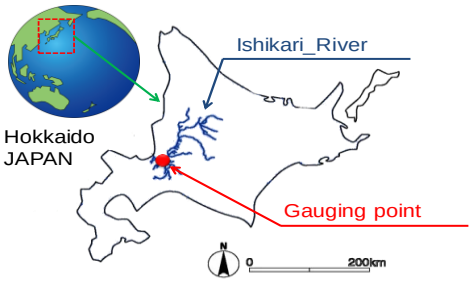

Figure 1. Gauging point

2.2 Observation system

Regarding the field observation, the authors used a human-crewed boat with tethering ADCP and MBES. The boat was equipped with a gasoline engine of 20 HP. The ADCP was tethered by wire rope of the boat side. MBES was installed on the side of the boat by steel pipes, as shown in Figure 2.

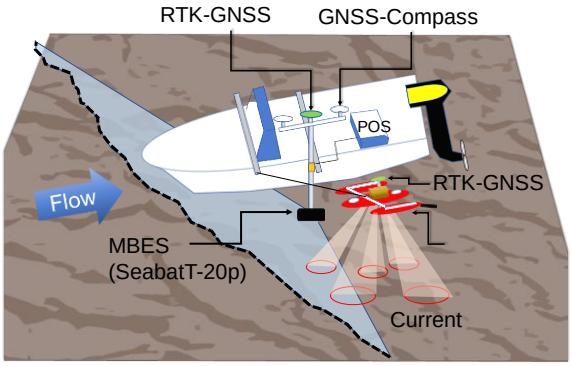

Figure 2. Observation system

2.3 ADCP

ADCP, River Pro ADCP manufactured by Teledyne RD Instruments, is mounted on a floating trimaran boat, as shown in Figure 2. Generally, ADCP has four slant beams with 20 degrees, and frequency is 1200 kHz. It measures the water velocity profiles, the water depth of four slant beams, and the surface riverbed moving speed.

2.4 MBES

MBES, Seabat T20 manufactured by Teledyne Reson, is a Doppler sonar system using multi beams to monitor bathymetry. Seabat T20 has up to 256 beams with a frequency from 190 to 420 kHz. The maximum swath angle is 120 degrees. MBES is controlled by the POS(Position and Orientation System). The accuracy is 0.02 degrees for the heading, 0.6cm for depth resolution, and 2cm for positional accuracy. Also, time was synchronized by GNSS. The conceptual figure relating to the monitoring of the riverbed by ADCP and MBES is shown in Figure 2.

2.5 Sediment sampling

Sediment sampler; Kumada dredge sampler is shown in Figure 3 was used to collect the river bed material. The sampler fixed by rope was dropped from the ship and drag either pulling by the hand or moving the boat to let the sampler dig the river bed. After that, the sampler was pulled up on the ship to collect the sediment. This can be considered as the bed material on the bed surface. Grain size analysis was performed on the accumulated sediment by a laser diffraction analysis method.

Figure 3. Kumada Dredge sampler

2.6 Water Surface slope

As water level gauges, we used "S & D mini" manufactured by Oyo corporation. The measurement interval was 10 minutes. The three water level gauges were installed at three locations from upstream to downstream, shown in Figure 6. The upstream was "WL1", the midstream was "WL2", and the downstream was "WL3". Also, the total distance from WL1 to WL3 was 1238.56m. Figure 5 shows the hydrograph of this flood as well as the duration of the observation. The

Figure 4. Water level gauge

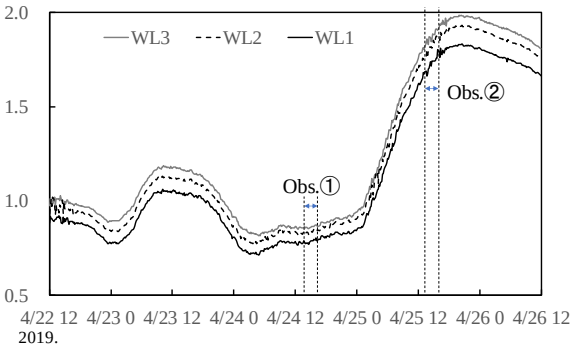

Figure 5. Hydrograph in Ishikari River

observation stage were two water level stages, "Obs.①" and "Obs.②". "Obs.①" was from 0.85m to 0.87m and "Obs.② "was from 1.83m to 1.92m.

2.7 Measurement strategy

First, using the difference between GNSS ship tracking and ADCP bottom tracking, we chose where the bed moves. The area was the range of the longitudinal section of 50 m and the transverse section of 10 m, as shown red line in Figure 6. The boat with the acoustic device was moved from downstream to upstream repeatedly every 10 minutes during 1.5 hours at a speed of about 0.7m/s. In detail, for "Obs.①", it was measured 13 times for 10 minutes every from 13:30 to 15:00 on April 24, and for "Obs.②", it was measured 13 times for 10minutes every from 13:30 to 15:00 on April 25.

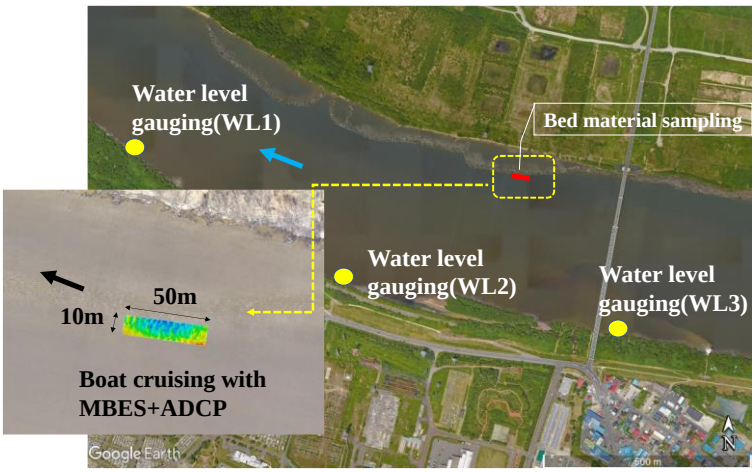

Figure 6. MBES and ADCP observation area and the sediment sampling point

3. Result of observation

3.1 Sand waves form

The contour map of the river bedforms obtained by MBES showed in Figure 7 and Figure 9. Also, Figure 8 and Figure 10 showed in longitudinally extracting the bed height of the central "selected line" in Figure 7 and Figure 9. As a result, the bed migration was small at "Obs.①", although the bed migration was clearly toward the downstream at "Obs.②".

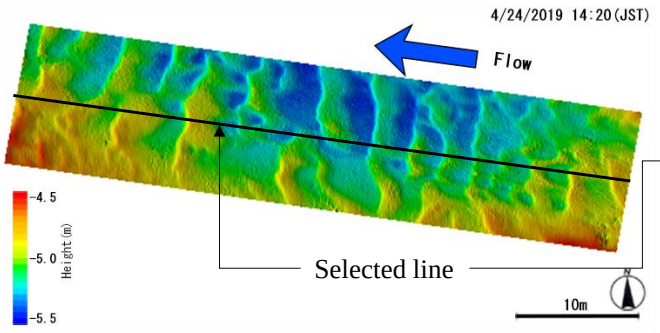

Figure 7. Bed form distribution (Obs.①)

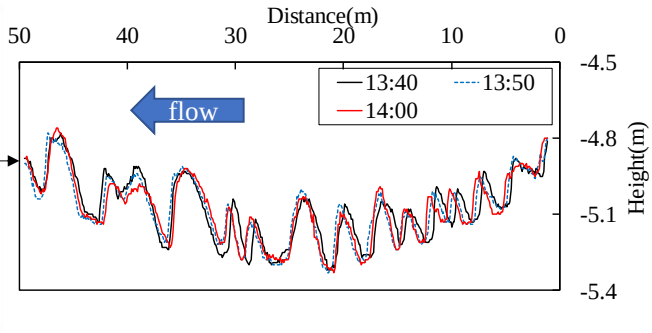

Figure 8. Sand wave distribution and migration (Obs.①)

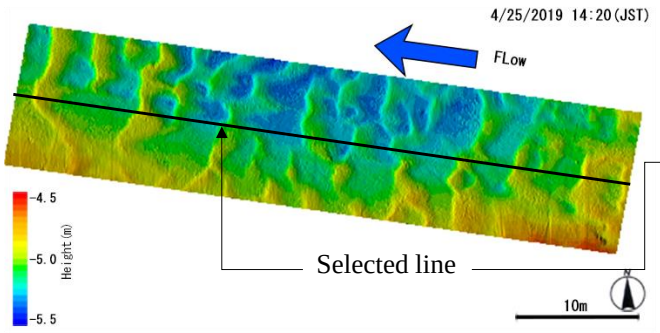

Figure 9. Bed form distribution (Obs.②)

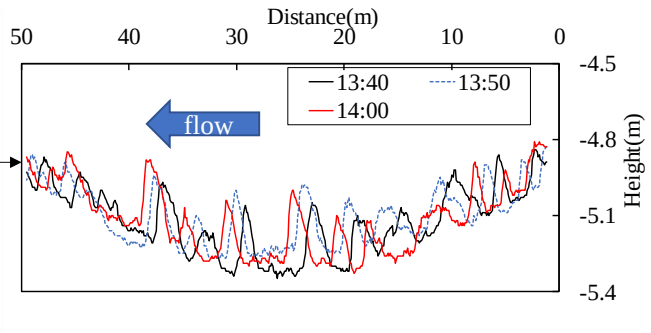

Figure 10. Sand wave distribution and migration (Obs.②)

3.2 Sand waves migration

Figure 11 and Figure 12 are plotted with the same data set in Figure 7 and Figure 9 but in a different format. This figure showed the Space-Time Image Velocimetry (STIV) method, which is firstly introduced by Fujita (2007). They are the contour plot of the river bed elevation, whose vertical axis is elapsed time and the horizontal axis are the distance of the selected lines in Figure 7 and 9. If the sand wave moves along the selected line with time, it can be shown as a diagonal line in this space-time image. Here, we traced the movement of the crest of the sand wave as a dotted black line. In our observation, we assume that the same altitude at a different time is the result of the movement of sand waves. Therefore, this phenomenon shows the migration of sand waves, and this slope of STI indicates the moving speed of the sand wave. The speed showed that 0.03m/min(=0.0005m/s) for "Obs.①", 0.11m/min(=0.0018m/s) for "Obs.②".

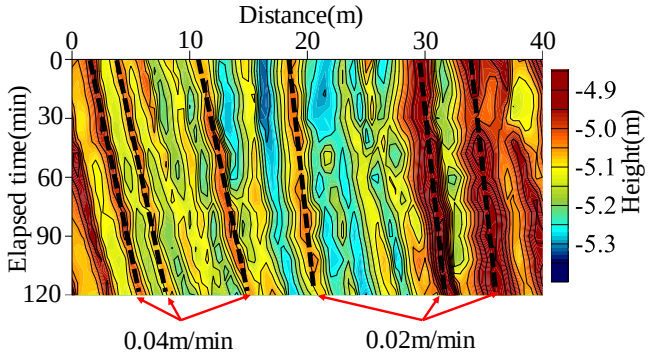

Figure 11. Sand wave moving speed calculated by STIV method (Obs.①)

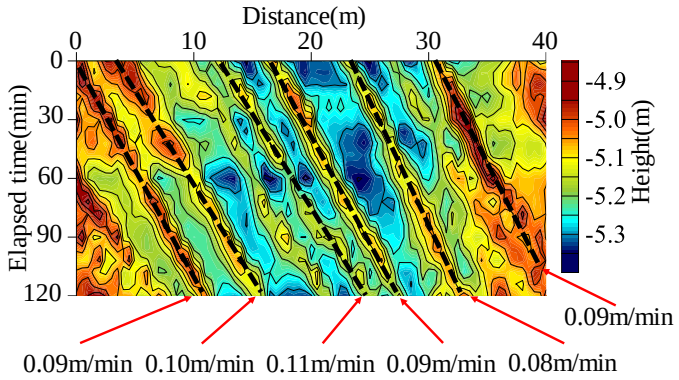

Figure 12. Sand wave moving speed calculated by STIV method (Obs.②)

4. RELATION BETWEEN DIMENSIONLESS SHEAR STRESS AND SAND WAVES

4.1 Dimensionless shear stress

We compared the two types methods of shear velocity(u_*① and u_*②). The dimensionless shear stress① was calculated by Eq. (1). The first method was to use water surface slope (I_e) and hydraulic radius(R) in Eq. (2).

$$\tau_*① = \frac{u_*^2①}{(\sigma/\rho - 1)gd} \tag{1}$$

$$u_*① = \sqrt{gRI_e} \tag{2}$$

where, τ_*=dimensionless shear stress; u_*=shear velocity; σ=mass density of sediment particles; ρ=mass density of water; g=acceleration gravity; d=size of particle; R=hydraulic radius; I_e=water surface slope

The second method was based on the Egashira (1997) in Eq. (3) to (9). The bedload velocity(u_b) was measured by the bottom tracking of ADCP and boat tracking of GNSS. The averaged sediment transport velocity(u_s) by bedload thickness is expressed in Eq.(4). According to Egashira et al. (1991), an approximate formula for the vertical velocity in a sandbed is proposed in Eq.(5). Also, It represents "$u(1)=u_b$" at the surface of bedload layer "$z=0$" and the averaged value "$u(z)$" calculated from the theoretical bed "$z=0$" to "$z=1$" at 0.1 intervals. Therefore, the coefficient α_{bs} is calculated 0.65 from Eq. (5). The coefficients were theoretically obtained that k_1 was related to the slope, k_2 was to relative water depth, f_d was to the particle collision, f_f was to the pore water. Also, h_w was the average water depth by ADCP. θ was the bed slope, which indicated the slope in the mean flow direction of the four beams of ADCP.

$$\frac{u_s}{u_*②} = \frac{4}{15}\frac{k_1 k_2}{\sqrt{f_d + f_f}}\tau_*② \tag{3}$$

$$u_s = \alpha_{bs} \cdot u_b \tag{4}$$

$$\frac{u(z)}{u_*②} = A_s\left[1 - \frac{h_s - z}{h_s}\right]^{3/2} \tag{5}$$

$$k_1 = \frac{1}{\cos\theta\{\tan\varphi_s/(1+\alpha) - \tan\theta\}} \tag{6}$$

$$k_2 = \frac{1}{c_s}\left[1 - \frac{h_s}{h_w}\right]^{1/2} \tag{7}$$

$$f_d = k_d(1 - e^2)(\sigma/\rho){c_s}^{1/3} \tag{8}$$

$$f_f = k_f(1 - c_s)^{5/3}{c_s}^{-2/3} \tag{9}$$

where, u_s = averaged sediment transport velocity by bedload thickness(u_s=α_{bs}×u_b); α_{bs}=correction coefficient for calculating u_s from u_b (=0.65) ; u_b= surface bedload velocity by ADCP; z=height from the theoretical bed height; A_s=function of c_s, θ , φ_s ; k_d =0.0828; k_f = 0.16; e = 0.85 coefficient of restitution; h_w = water depth; φ_s=interparticle friction angle; θ=bed slope by ADCP; α = 0.25 dynamic pressure/static pressure; c_s =averaged sediment concentration by bedload thickness (h_s). Regarding the c_s, the concentration of the surface of the bedload (z = h_s) is zero. The concentration of static soil of particles at the upper-end (z = 0) is 0.6 using 0.4 of the porosity in the fixed ground. Because the distribution of static soil particle in the layer is approximately linear, c_s is valued 0.6/2 = 0.3.

4.2 Relation between dimensionless shear stress and wave steepness

Yalin(1978) proposed the relation between dimensionless τ_* and wave steepness H/L(H=wave height, L=wavelength). In order to compare the result of two types of u_*, the measured data were plotted on the Yalin's diagram in Figure 13. Figure13(a) was to use water surface slope (I_e) and hydraulic radius(R) in Eq. (2). Figure 13(b) was based on the Egashira(1997) in Eq. (3) to (9). Figure13(b) was plotted as spreading out than Figure13(a). The reason is that τ_* was calculated using the bedload velocity by ADCP. The critical tractive force(τ_{*c}) was used 0.04 for previous experimental data obtained by Iwagaki's equation(1956). The size of the particle was d60=0.93 mm. Both the calculation method of dimensionless shear stress indicated good agreement with the curve constructed by Yalin. However, the diagram of (b) was plotted as spreading out than the diagram of (a). The reason is that τ_*② was calculated using the bedload velocity by ADCP. Regarding "Obs.②", H/L tended to decrease, although τ_*/τ_{*c} tended to increase. This result was consistent with the observation result by MBES, which is despite the high water level, the wave height was decreased.

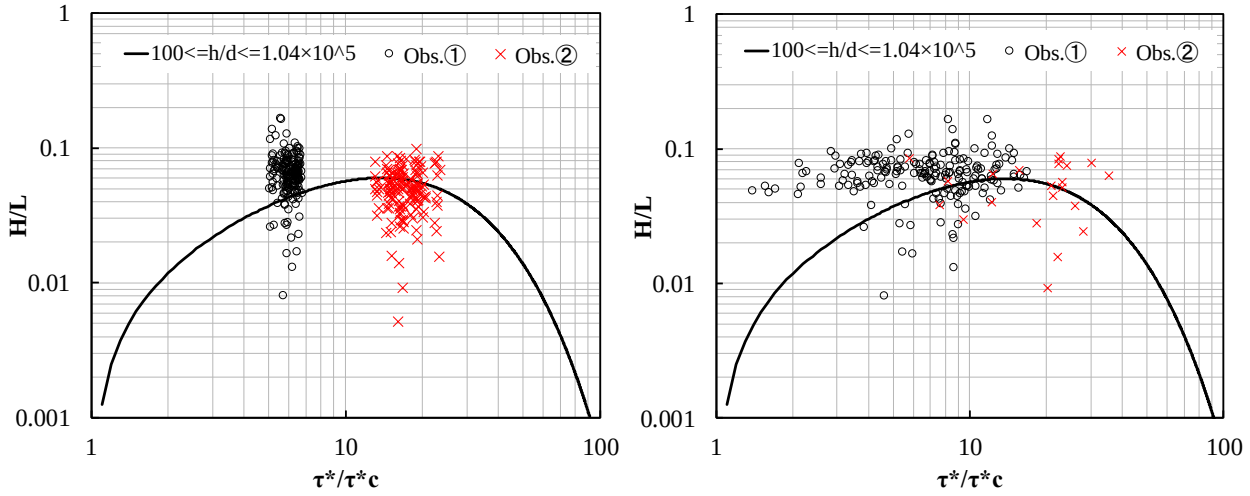

(a) Water surface slope and water depth as Eq.[2] (b) Egashira et al. Eq.[3]-[9]

Figure 13. Relation between τ_*/τ_{*c} and H/L proposed by Yalin(1978)

4.3 Relation between dimensionless shear stress and flow resistance

The flow resistance was analyzed from the theory of Kishi & Kuroki(1973) and the method of Kudo et al. (2016). Kishi & Kuroki(1973) proposed the relation between τ_* and bedform drag τ_*'. Figure 14 shows the relationship between τ_* and τ_*' using "Obs.①" and "Obs.②". As a result, the following was found. Firstly, for the both of "Obs.①" and "②", τ_*' was plotted on the line of Dune. Secondly, it was tended that τ_*' increased as τ_* increased. Thirdly, it was suggested both of "Obs.①" and "②" did not reach the stage where the occurrence of transition.

4.4 Sand wave form and relation between τ_*① and τ_*②

The change of the sand waveform and the relation of flow resistance in time series showed in Figure 15., Figure 16. and Table 1. These are the results at the same location, 50m in the longitudinal direction, and 10m in the transverse direction. The hydraulic condition was different between "Obs.①" and "Obs.②". The water level of "Obs.②" was 1m higher than "Obs.①". For the sand wave features, the wavelength of "Obs.①" was 3.10m on average, and "Obs.②" was 3.64m on average, "Obs.②" was slightly longer than "Obs.①". The wave height was the same at 0.2m each other. The ratio of wave height to wavelength was 0.05-0.06. The number of waves at the low water level("Obs.①") was higher than the number of waves at the high water level("Obs.②"). In particular, the latter of "Obs.②", the number of waves increased as the water level was rising, but the wavelength tended to be short. During the observation, the dimensionless shear stress in the range of τ_*=0.2～0.8 was observed. Regarding the flow, resistance was observed as follows. τ_* on average of "Obs.①" was τ_*①=0.24 and τ_*②=0.30. τ_* on average of "Obs.②" was τ_*①=0.66 and τ_*②=0.80. Regarding τ_*① and τ_*②, there was a small difference at "Obs.①". When the dimensionless shear stress is small, the hydraulic phenomenon occurring inside the river bed wave can be represented by Eq.(1). Still, when the dimensionless shear stress increases, local phenomena prevail. Therefore, it can be inferred the method of Eq.(3) is more representative than Eq. (1). A sand wave moving speed of bedform becomes large as τ* becomes large. However, the sand wave height was the same order. Therefore, the sand wave height did not follow the same trend as the sand wave moving.

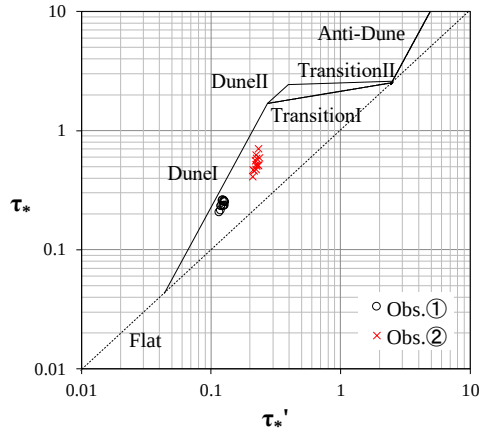

Figure 14. Relation between τ_* and τ_*' proposed by Kishi&Kuroki(1973)

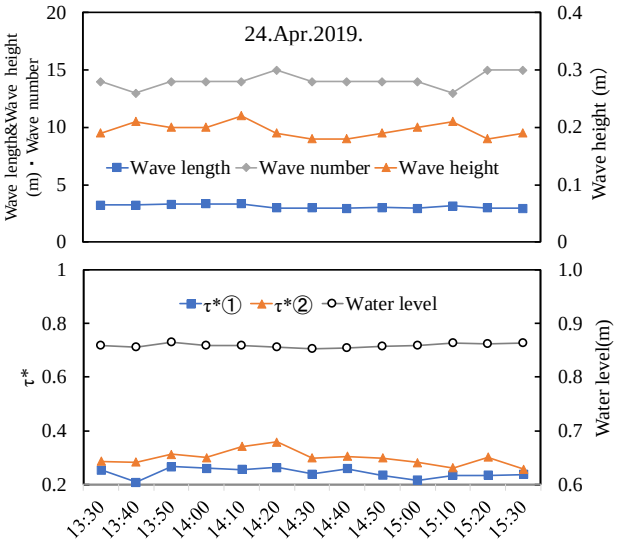

Figure 15. Sand wave form and τ_* (Obs.①)

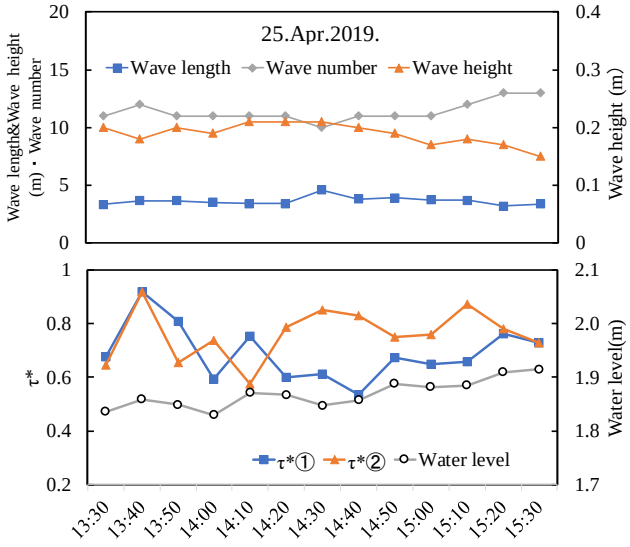

Figure 16. Sand wave form and τ_* (Obs.②)

Table 1. Sand wave form feature

No.	date	time	Number of sand wave	Water level (m)	Average wave length (m)	Average wave height (m)	Wave height/Wave length	τ*①	τ*②	d60 (mm)
Obs.①	2019/4/24	13:30-15:30	14	0.85～0.87	3.10	0.20	0.06	0.24	0.30	0.93
Obs.②	2019/4/25	13:30-15:31	11	1.83→1.92	3.64	0.19	0.05	0.66	0.80	0.93

5. BEDLOAD DISCHARGE CALCULATION

5.1 Equations of bedload discharge

In order to estimate the bed load discharge, two types of bedload discharge equations were implemented. The first one(q_b①) is the bed form migration, which is the function of the wave height and the wave speed proposed by Kikkawa (1985) as shown in Eq.(10). The bedload discharge was calculated from the moving speed of the sand wave on the longitudinal line and the wave height of the crest. The second one (q_b②) is the method of bedload discharge based on equations of Egashira (1997) proposed by Koseki et al. (2016), as shown in Eq.(11) ～(13). Eq.12 expresses the ratio of the thickness of the total sand layer to the entire flow layer. Also, Eq.12 can be transformed into Eq.13.

$$q_b① = (1-\lambda)H \cdot U_w \tag{10}$$

where, q_b=bedload discharge; λ=porosity of sediment (=0.4 used); H=height of sand wave
U_w=moving speed of sand wave

$$q_b② = \int_0^{h_s} c \cdot u \cdot dz \cong \alpha_{bs} \cdot u_b \cdot h_s \cdot c_s \tag{11}$$

$$\frac{h_s}{h_t} = \frac{2\tan\theta}{\left(\frac{\delta}{\rho}-1\right)c_s\{\tan\varphi_s/(1+\alpha)-\tan\theta\}} \tag{12}$$

$$\frac{h_s}{d} = \frac{1}{c_s\cos\theta\{\tan\varphi_s-\tan\theta\}}\tau_* \tag{13}$$

where, q_b=bedload discharge; αbs=0.65 correction coefficient for calculating u_s from u_b by ADCP; u_b=bedload velocity by ADCP; h_s=bedload thickness; α = 0.25 dynamic pressure/static pressure; c_s=averaged sediment concentration by bedload thickness (h_s); h_t= thickness of total flow layer (h_t=h_s+h_w) ; h_w = thickness of water flow layer measured by ADCP ; δ =density of sand; ρ =density of water ; d= sediment particle size(=d60); φ_s=interparticle friction angle; θ=bed slope by ADCP; τ_*=dimensionless shear stress

5.2 Result of bedload discharge

The bedload discharge was calculated using two samples (“Obs.①”, “Obs.②”) using the equation of Kikkawa(1985) using MBES and Koseki et al. (2016) using ADCP as shown in Table 2. As a result, the two types of bedload discharge were almost the same order. However, there were some differences in the bedload discharge by two methods especially low water level. Also, in this field observation, there were no bedload samples to compare with, unfortunately. It is necessary to further analysis and fieldwork near future.

Table 2. Bedload discharge

No.	date	**Kikkawa(1985) (×10^{-3}m^3/S/m)**	**Koseki(2016) (×10^{-3}m^3/S/m)**
Obs.①	**2019/4/24**	0.06	0.03
Obs.②	**2019/4/25**	0.21	0.28

6. CONCLUSIONS

1) In this study, the authors conducted field observation using MBES, ADCP, and sediment sampling to measure bedforms, sand wave migration, and bedload velocity at the same time in the actual river. We succeeded in measuring several sand waves and their migration.
2) Two-stage of different water levels were measured shape of the sand wave, and the averaged wave height was 0.19-0.20 m, while the averaged wavelength was 3.10-3.64 m, which gives the wave height/wavelength of 0.05-0.06.
3) River bed migration from 0.03 m/min(=0.0005 m/s) to 0.11 m/min(=0.0018m/s) was estimated as sand wave moving speed using STIV(Space-Time Image Velcimetry) method.
4) Sand wave moving speed of bedform becomes large as τ* becomes large. However, as the sand wave height was the same order, it was found that the sand wave height did not follow the same trend as a wave moving speed.
5) Observed flow resistance was similar to what can be obtained by Kishi &Kuroki(1973), and the results showed good agreement with the curve constructed by Yalin (1978).

6） Regarding the bed load discharge, two different methods were compared. The bedload discharge was calculated using two samples (“Obs.①”, “Obs.②”) with equations of Kikkawa(1985) using MBES and method of Koseki et al. (2016) using ADCP. Two types of bedload discharge were almost the same order.

ACKNOWLEDGMENTS

We would like to express our gratitude to the Sapporo Development and Construction Department, Hokkaido Reginal Development Bureau, for the great help of field study.
Mostly, I would like to deepest gratitude to Dr. Atsuhiro Yorozuya (The International Centre for Water Hazard and Risk Management under the auspices of UNESCO) for valuable advice and teaching us to complete this study.

REFERENCES

A. Shields(1936), Anwendung der Ähnlichkeitsmechanik und der Turbulenzforschung auf die Geschiebebewegung, Mitteilung der Preussischen Versuchsanstalt für Wasserbau und Schiffbau, Heft 26, Berlin.

Abraham, D., T. C. Pratt, and J. Sharp (2010), Measuring bedload transport on the Missouri River using time sequenced bathymetric data, 2nd Joint Federal Interagency Conference, Las Vegas, Nev. (available at http://acwi.gov/sos/pubs/2ndJFIC/HOME.pdf)

Abraham, D., R. A. Kuhnle, and A. J. Odgaard (2011), Validation of bed-load transport measurements with time-sequenced bathymetric data, J. Hydraul. Eng., 137(7), 723–728, doi:10.1061/(ASCE)HY.1943-7900.0000357.

A. Yorozuya, S. Okada, K. Ejima, Y. Kanno, and K. Fukami (2010), Method for Estimating Shear Velocity and Bedload Discharge with Acoustic Doppler Current Profiler, Annual Journal fo Hydraulic Engineering, JSCE, Vol.54, pp.1093-1098.

A.Uehara, S.Okada, A.Yorozuya, and H.Koseki (2018),Experimental study on the calculation method of the bed load discharge using the bottom track velocity measured by ADCP,Annual Journal of Hydraulic Engineering, JSCE, Vol.74,I_631-I_636.

Collin D. Rennie, Robert G. Millar, and Michael A. Church (2002), Measurement of Bed Load Velocity using an Acoustic Doppler Current Profiler, Journal of Hydraulic Engineering, MAY 2002, pp.473-483.

S. Egashira, K. Miyamoto, and T. Itoh(1997), Constitutive Equations of Debris-Flow and Their Applicability, Proc. of 1st International Conference on Debris-flow Hazards Mitigation,C. L. Chen (Eds.), ASCE: NewYork; pp. 340-349.

Engelund, F. (1967), Closure to “Hydraulic Resistance of Alluvial Streams.” Journal of the Hydraulics Division, ASCE,Vol.93, No. HY-4, pp.287-296.

G. Gerbi., J. Trowbridge, J. Edson, A. Plueddemann, E. Terray,and J. Fredricks (2008), Measurements of momentum and heat transfer across the air-sea interface. J. Phys.Oseanogr., 38, 1054-1072.

H.Koseki,A.Yorozuya,S.Kudo, and Y.Iwami (2016), Development of a system to measure bed forms and vertial velocity profiles in a river channel,River Flow 2016.

I. Fujita, H. Watanabe , and R. Tsubaki (2007), Development of a nonintrusive and efficient flow monitoring technique: The space time image velocimetry (STIV), International Journal of River Basin Management, Vol.5, No.2, pp.105-114.

Iwagaki, Y., (1956), "Hydrodynamical Study on Critical Tractive Force," Trans. Japan Society of Civil Engineering, No. 41.

K. Ashida, M. Michiue (1972), Study on Hydraulic Resistance and Bed-load Transport Rate in Alluvial Streams, ransactions of JSCE 206: 59-69.

Masahiro Hashiba, Koichi Tsuchida, Atsuhiro Yorozuya, and Hiroshi Koseki(2019), "Study of sand waves with ADCP and multi-beam echo-sounder in actual river", *International Symposium and Exhibition on Hydro-Environment Sensors and Software*, pp.128-135.

Muste, M., Baranya, S., Tsubaki, R, Kim, D., Ho, H-C., Tsai, h-W., and Law, D. (2015). “Acoustic Mapping Velocimetry Proof-of-concept Experiment,” Proceedings 36th IAHR World Congress, 28 June – 3 July, The Hague, The Netherlands.

Muste, M., Baranya, S., Tsubaki, R., Kim, D., Ho, H-C., Tsai, H-W., and Law, D. (2016). “Acoustic Mapping Velocimetry,” Water Resources Research, 52, doi:10.1002/2015WR018354.

R. Ramooz, C.D. , and Rennie(2010), Laboratory measurement of Bedload with an ADCP, US Geological Survey Scientific Investigations Report 2010-5091 : 367–386.

S. Egashira, K. Miyamoto, and T. Itoh (1997). Constitutive Equations of Debris-Flow and Their Applicability, Proc. of 1st International Conference on Debris-flow Hazards Mitigation, C. L. Chen (Eds.), ASCE: NewYork; pp. 340-349.

Yalin, M.S. and Karahan, F. (1978), Steepness of sedimentary dunes, Proc. ASCE, Vol.105, HY4, pp.381-392.